

Direct characterization of any linear photonic device

Saleh Rahimi-Keshari¹, Matthew A. Broome^{1,2}, Robert Fickler^{3,4},
Alessandro Fedrizzi^{1,2}, Timothy C. Ralph¹, and Andrew G. White^{1,2}

¹*Centre for Quantum Computer and Communication Technology,*

²*Centre for Engineered Quantum Systems, School of Mathematics and Physics,
University of Queensland, Brisbane, QLD 4072, Australia*

³*Quantum Optics, Quantum Nanophysics, Quantum Information, University of Vienna, A-1090, Austria*

⁴*Institute for Quantum Optics and Quantum Information, Boltzmannngasse 3, Vienna A-1090, Austria*

We introduce an efficient method for characterizing any multi-mode linear photonic network. Our method employs a standard laser source and intensity measurements to directly determine all moduli and non-trivial phases of the matrix describing the network. We experimentally demonstrate our method by characterizing a 6×6 fibre-optic network and independently verify the results via nonclassical two-photon interference.

PACS numbers: 03.65.Wj, 42.50.-p, 42.50.Ex

Implementation of quantum technologies requires the ability to realise arbitrary unitary operators, enabling applications such as efficient quantum simulation and computation. In principle, linear photonic devices can be used to experimentally realise any $N \times N$ unitary operator [1]. However, a significant remaining practical challenge is to characterize the device once it is built. A known solution is to perform full quantum process tomography of a device using nonclassical states [2–4] or coherent states [5, 6]. This standard approach however requires the full suite of quantum tools—such as N-mode quantum state preparation and measurement—and is, despite progress on more efficient methods such as compressive sensing [7], relatively slow and impractical for large interferometric devices.

A more tractable approach, starting from the assumption of linearity, is to adapt existing methods from classical optics. As a linear photonic circuit can always be cast as an interferometer with $(N^2 - N)/2$ beam-splitters [1], it can be fully characterized by embedding it in an external interferometer using a local oscillator [8]. The interferometric stability required is sufficiently challenging in practice that this is rarely done for quantum optics experiments. Recently, a method was proposed that obviates the use of an external interferometer; however, it requires nonclassical interference [9] for characterization of linear optical devices [10, 11].

Here we introduce a method to characterize the $N \times N$ matrix representing an N -mode linear photonic network using readily available standard laser source and photodetectors, and without using an external local oscillator. Our method eliminates the need for nonclassical interference and single-photon detectors; it is simple and efficient, requiring only $2N - 1$ configurations for directly measuring all nontrivial parameters of the $N \times N$ matrix. We demonstrate our method by characterizing an integrated device—a 6×6 fused-fibre coupler—and highlight its precision by comparing measured quantum interference patterns with those predicted using the classically-

estimated matrix.

A linear multi-mode photonic network can be represented by a matrix U that relates the creation operators of the input and output modes

$$b_k^\dagger = \sum_{j=1}^N U_{jk} a_j^\dagger. \quad (1)$$

For an ideal lossless network the matrix U is unitary, but in practice, due to loss, it is a submatrix of a unitary matrix. Notice that the knowledge of U simply determines the action of the network on any multi-mode coherent states, and in principle following the method presented in Ref. [6], one can predict the output state of the network for any given input state. However, for a network with a large number of modes, this task is believed to be computationally hard for certain input states [12].

Generally, the elements of the matrix U are complex numbers $U_{jk} = r_{jk} e^{i\theta_{jk}}$, where $0 \leq r_{jk} \leq 1$ and $0 \leq \theta_{jk} < 2\pi$. Noting that the phases of the basis vectors are not physically significant, we can absorb $(2N - 1)$ phases into the basis vectors [13]. Thus, any matrix U can be decomposed as a product of three matrices $U = D(\mu) U' D(\nu)$, where $D(\mu) = \text{diag}(e^{i\mu_1}, e^{i\mu_2}, \dots, e^{i\mu_N})$ and both U and U' describe the same physical process. Without loss of generality, we let $\theta_{1j} = \theta_{j1} = 0$, for $j = 1, 2, \dots, N$, and we are left with $(N - 1)^2 + N^2$ free parameters to be determined in the characterization.

Even if U is unitary, it has been shown that knowledge of all moduli r_{jk} —where r_{jk}^2 is the probability of detecting a photon at the output port k when only one single photon was sent to the input port j —does not uniquely determine all phases for $N > 3$ [13, 14]. Therefore, in order to characterize the matrix U , in general, we require probe states and measurements that are sensitive to the phases θ_{jk} .

One way to achieve that, as shown in [10, 11], is to insert two single photons into different input modes and to record nonclassical interference patterns between

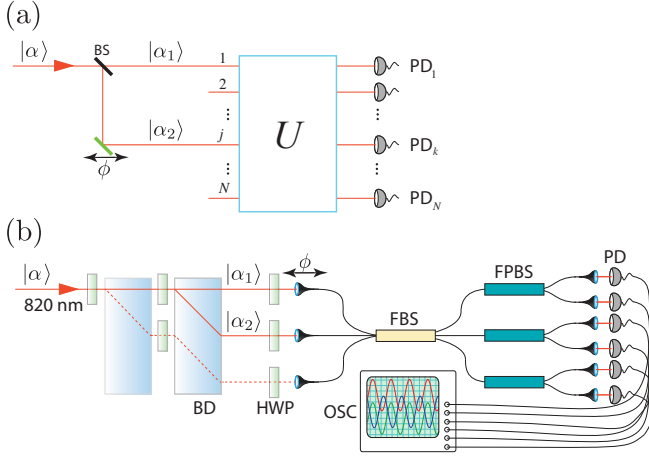


FIG. 1: Scheme for characterizing any linear photonic device, U . (a) Using a 50:50 beam-splitter (BS) and phase shifter (ϕ) a dual-mode coherent state, $|\alpha\rangle$, is prepared and sent through U , where $\alpha_2 = e^{i\phi}\alpha_1$. By sequentially inputting $|\alpha_2\rangle$ into modes 2, 3, ..., N , and varying the phase over at least 2π , all phases of matrix U can be directly measured using photodiodes (PD). (b) Experimental realisation. The device-under-test is a 3×3 -mode fused-fibre beam-splitter (FBS), which constitutes a 6×6 photonic network when polarization is included. Orthogonal polarisation modes are resolved using fibre polarization beam-splitters (FPBS) at its outputs. Interferometric probe states between pair-wise input combinations are prepared with two polarization beam displacers (BD), and half-wave plates (HWP). Our bulk optics method to direct coherent states here is used for convenience only. Finally, the outputs are monitored with fast photo-diodes connected to an oscilloscope (OSC) while the phase ϕ is scanned with a motorised linear micro-translation stage.

different combinations of output modes. Alternatively, the nonclassical interference can be simulated using two-mode coherent states with randomized relative phases, but at the cost of an increased level of noise and reduced classical interference visibility [15, 16]. Our method takes a more direct route, only requiring a standard laser source, split at a beam-splitter, with a varying relative phase between the resulting dual-mode coherent state; see the experimental setup in Fig. 1(a). An interesting feature of this method is that it enables us to measure all the nontrivial phases of the matrix U directly without solving any trigonometric equations. It thus significantly simplifies the task of characterization.

Our method works as follows (details of the algorithm can be found in the Appendix):

1. Send coherent state of light into the N input modes individually, and measure the output r_{jk}^2 of all $k=1, 2, \dots, N$ outputs modes for every input j . From this, obtain r_{jk} .
2. Prepare a dual-mode coherent state into pairwise input combinations between input 1 and the input $j=2, 3, \dots, N$, with a variable phase ϕ . Measure

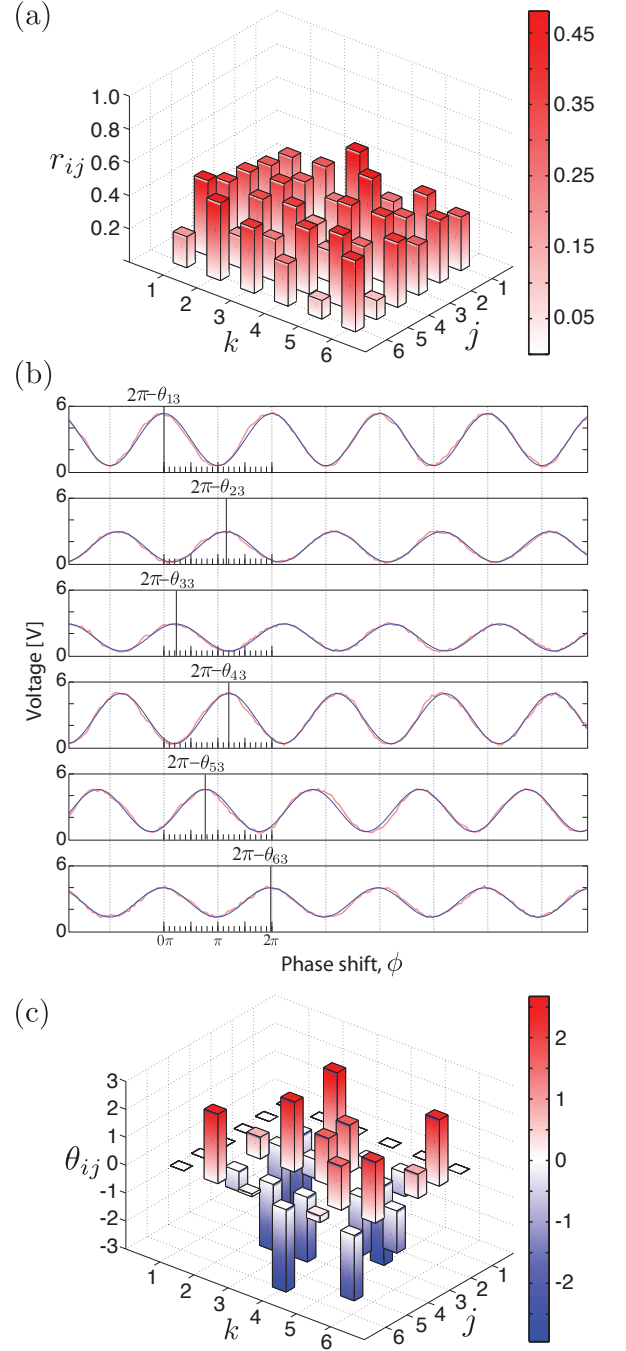


FIG. 2: Experimental characterization of a linear photonic device. (a) The moduli r_{jk}^2 of the experimentally measured U_{exp} . The x and y axes correspond to the input and outputs modes, j and k respectively. (b) Representative experimental data for obtaining θ_{jk} . Injecting coherent state of light into input modes 1 and 3 of the 6-mode device. The amplitudes (voltage at output photo-diodes) of the six output modes (1-6 from top-to-bottom) oscillate as the phase ϕ is swept in time. The red and blue lines are measured data and theoretical fits to $A \cos(\phi - \theta_{jk})$ respectively. (c) All phases θ_{jk} of the measured matrix U_{exp} . The entire characterization method was performed 10 times to obtain experimental uncertainties, however in all plots the experimental uncertainties are not visible on the scales shown.

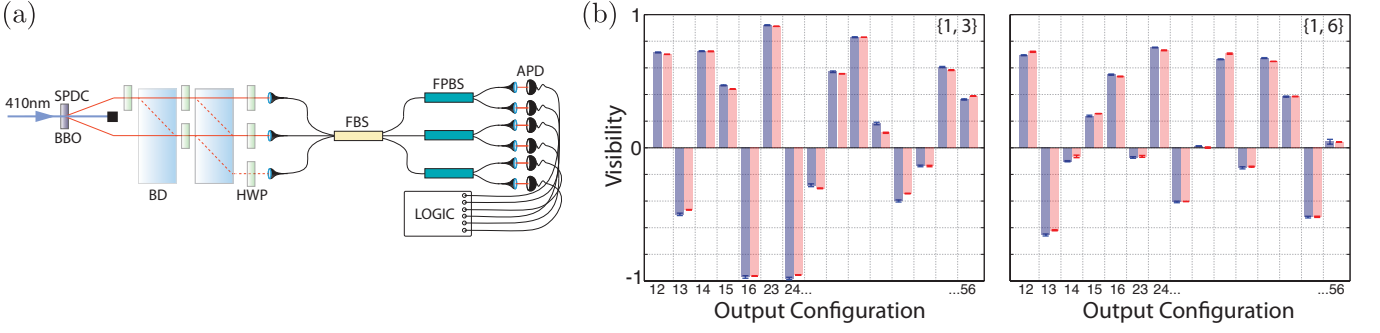


FIG. 3: Independent verification of the measured matrix U_{exp} . (a) Experimental schematic. A pair of photons is generated via spontaneous parametric downconversion (SPDC) in a nonlinear beta-barium-borate (BBO) crystal pumped with a mode-locked pulsed laser at 410 nm with type-I phase matching to produce polarization degenerate photons at 820 nm. After being spectrally filtered (FWHM 2 nm) the individual downconverted photons are steered into the optical modes of the linear photonic network by a series of beam displacers (BD) and half-wave plates (HWP). Upon passing through the photonic circuit the photons are detected using avalanche photo-diodes (APD) who's coincident signals are monitored using a commercially available counting logic. (b) Measured nonclassical visibilities vs. predicted visibilities are shown in the left and right panels are for photons input into modes $\{1, 2\}$, and $\{1, 6\}$ respectively. The red bars show the directly measured nonclassical visibilities, the blue bars show the predictions from the measured matrix U_{exp} , and errors are given at the top of each data point. The numbers on the x-axis show the corresponding output modes for which that nonclassical interference is measured.

the output intensities of all modes $k=1, 2, \dots, N$ as a function of ϕ . This yields all non-trivial phases θ_{jk} .

We tested our method by characterizing a fused fibre-optic beam-splitter, the experimental setup is shown in Fig. 1(b). The network itself is composed of one 3×3 non-polarizing fused fibre-optic beam-splitter (FBS) with three 2×2 orthogonally-polarizing beam-splitters at each of its output modes. By mapping onto orthogonal polarizations at the input of the initial FBS the whole network is described by a 6×6 matrix U_{exp} . The input modes are labelled $\{1, 2, \dots, 6\} = \{|H\rangle_1, |V\rangle_1, |H\rangle_2, \dots, |V\rangle_3\}$, where $|H\rangle_1$ is the horizontally polarized mode for spatial mode '1' of the FBS.

In the setup we used a series of polarization beam displacers and half-wave plates to prepare input probe states, allowing for phase-stable interferometric measurements and polarization control for the input of the FBS. The phase ϕ was controlled by a motorised linear micro-translation stage at input mode '1' to introduce an optical path difference of 0.1 mm, at a speed of 0.05 mm/s, between two inputs. Scanning over this short time window limits the effect of thermal drift on the classical interferometer, therefore removing the need for active locking. The outputs were coupled to fast photodiodes and monitored simultaneously on an oscilloscope while the phase ϕ was scanned. All characterization measurements were performed with a 100 μW laser diode filtered to have a centre wavelength of 820 nm and a full-width half-maximum bandwidth of 2 nm.

We first measured the 36 output intensities for the six individual inputs shown graphically in Fig. 2(a). We then recorded interference fringes for the pair-wise input combinations discussed above, and fitted sinusoidal curves to

the resulting photocurrents to obtain experimental values for θ_{jk} (see Appendix for details), see Fig 2(b) and (c). From these measurements, we reconstructed the 6×6 matrix U_{exp} .

We verify our experimentally obtained matrix U_{exp} by measuring two-photon interference inside the linear optical network [9]. As this is a fourth-order interference effect, it provides a suitable independent verification for the validity of U_{exp} which we obtained with our second-order interference method. We created and sent two single-photons into the 6×6 network, and measured the coincidences at all fifteen (6 choose 2) pairwise combinations of output modes using the experimental setup shown in Fig. 3(a). The nonclassical visibility is calculated as $(C_{\text{out}} - C_{\text{in}})/C_{\text{out}}$ where C_{in} and C_{out} are the coincidence count rates of photon pairs at the outputs of

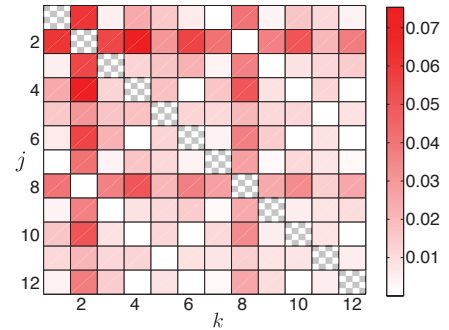


FIG. 4: The matrix $V_{\text{exp}} V_{\text{exp}}^\dagger$. The diagonal hatched squares are equal to unity by construction (see Appendix) and the off-diagonal elements are coloured according to their value given by the color bar on the right.

the circuit inside (maximum temporal overlap between photons) and outside (no overlap) the interference dip, respectively. The results for two different input configurations are shown in Fig. 3(b). The obtained interference patterns are in excellent agreement with those predicted by U_{exp} .

Having verified our method, we will now discuss how U_{exp} —which we do not expect to be a unitary matrix because of inevitable loss—can be embedded into a larger matrix which will more closely approximate a unitary matrix. Assuming the optical loss is equal for different paths connecting specific inputs to outputs, we can model this loss as virtual beam-splitters on the input modes. With this we obtain the 12×12 matrix V_{exp} following the algorithm described in the Appendix. If our linear photonic device satisfied these assumptions, we would expect V_{exp} to be unitary. A simple measure of this unitarity is to check how close $V_{\text{exp}} V_{\text{exp}}^\dagger$, given in Fig. 4, is to identity. In our case $V_{\text{exp}} V_{\text{exp}}^\dagger$ has non-zero but very small off-diagonal elements. This is indicative of both inevitable experimental uncertainty in the measured matrix elements and the effect of *path-dependent* loss in the linear optical network.

The question remains as to what unitary best describes the linear optical network. It has been shown that the closest unitary matrix to V_{exp} can be found by using the polar decomposition $\tilde{U} = (V_{\text{exp}} V_{\text{exp}}^\dagger)^{-\frac{1}{2}} V_{\text{exp}}$ [17]. The resulting unitary matrix \tilde{U} does not noticeably alter the predicted two-photon interference visibilities of Fig. 3(b), and therefore describes our device with a good approximation.

As photonic quantum technologies mature beyond small-scale proof-of-principle demonstrations [18–20], there is increasing requirement for improved methods for full tomography, process validation and verification. Areas of direct applicability include the experimental characterization of large linear waveguide arrays for photonic quantum walks [21, 22], especially those built in 3D where current approaches using top-down imaging are not possible [23]. One of the most exciting applications for larger systems pertains to an intermediate model of quantum computation—namely, that of BOSONSAMPLING [12]. Our method provides an efficient means for characterizing large linear optical networks to obtain the scattering probabilities of multi-photon processes, which is a crucial component of a photonic BosonSampling experiment. For these larger characterizations a many-mode optical switch board built into inherently stable integrated wave-guide circuits [24] could be used to prepare and steer the required dual-mode coherent states, as opposed to a larger bulk-optics setup. A simpler way to achieve the required small displacements is to tilt optical components in the probe beam path [16].

We thank Devon Biggerstaff, Shahla Nikbakht, and

Peter Rohde for discussions. This work was supported in part by: Centre for Quantum Computation and Communication Technology (CE110001027), Centre for Engineered Quantum Systems (CE110001013), the Australian Research Council’s Federation Fellow program (FF0668810), and the SFB program W1210-2 (Vienna Doctoral Program on Complex Quantum Systems - CoQuS) of the Austrian Science Fund (FWF); and the University of Queensland Vice-Chancellor’s Senior Research Fellowship program.

Appendix

Here we show how to construct the matrix V_{exp} (labelled V here for neatness) directly from the experimental measurements. We model a lossy $N \times N$ linear photonic device by adding virtual beam-splitters with transmissivities η_j ($0 \leq \eta_j \leq 1$) to each input of an $N \times N$ unitary matrix with elements $U_{jk} = r_{jk} e^{i\theta_{jk}}$, and the resulting $2N \times 2N$ unitary matrix is given by

$$V = \begin{pmatrix} \eta U & -\tilde{\eta} \\ \tilde{\eta} U & \eta \end{pmatrix}, \quad (\text{A.2})$$

where

$$\eta = \text{diag}(\eta_1, \eta_2, \dots, \eta_N),$$

$$\tilde{\eta} = \text{diag}\left(\sqrt{1 - \eta_1^2}, \sqrt{1 - \eta_2^2}, \dots, \sqrt{1 - \eta_N^2}\right).$$

Using Eq. (1), the output amplitudes of a general N -mode input coherent state $|\alpha_1, \alpha_2, \dots, \alpha_N\rangle$ are given by

$$\beta_k = \sum_{j=1}^N V_{jk} \alpha_j. \quad (\text{A.3})$$

We can thus send a coherent state with known intensity I to input port j , where all other input modes are in vacuum state, and measure the intensity from all output ports simultaneously

$$I_k = I (\eta_j r_{jk})^2, \quad k = 1, 2, \dots, N. \quad (\text{A.4})$$

We also have

$$(\eta_j)^2 = \frac{1}{I} \sum_{k=1}^N I_k. \quad (\text{A.5})$$

Thus using equations (A.4) and (A.5) for $j=1, 2, \dots, N$ all the moduli r_{jk} can be obtained.

The next step is to measure all nontrivial phases using two-mode coherent states. We send a coherent state $|\alpha\rangle$ to a 50:50 beam-splitter and use a phase shifter to control the relative phase between the output states $|\alpha_1\rangle$ and $|\alpha_2\rangle$ with the same intensity I ; see Fig. 1(a). We send

$|\alpha_1\rangle$ to input mode ‘1’ and $e^{i\phi}|\alpha_2\rangle$ to input port j . The intensities of the output coherent states are given by

$$I_k = I |V_{1k} + V_{jk} e^{i\phi}|^2. \quad (\text{A.6})$$

As all elements in the first row and the first column are real, the above equation becomes, for $k \neq 1$

$$\begin{aligned} I_k &= I \left| \eta_1 r_{1k} + \eta_j r_{jk} e^{i(\phi + \theta_{jk})} \right|^2 \\ &= I \left[(\eta_1 r_{1k})^2 + (\eta_j r_{jk})^2 + 2\eta_1 \eta_j r_{1k} r_{jk} \cos(\phi + \theta_{jk}) \right], \end{aligned} \quad (\text{A.7})$$

and for $k=1$

$$I_1 = I \left[(\eta_1 r_{11})^2 + (\eta_j r_{j1})^2 + 2\eta_1 \eta_j r_{11} r_{j1} \cos(\phi) \right]. \quad (\text{A.8})$$

When I_1 attains its maximum value we have $\phi=0$, and $\phi=\pi$ for its minimum value. This serves as our reference mode, and without loss of generality we always choose I_1 at its maximum for our reference of $\phi=0$. Having this capability, we further sweep ϕ until I_k attains its maximum value (see Fig. 2(b)) and using Eq. (A.7) the unknown phases can be found as

$$\theta_{jk} = 2\pi - \phi. \quad (\text{A.9})$$

Therefore, by repeating this procedure for $|\alpha_2\rangle$ input into mode $j=2, 3, \dots, N$ all the nontrivial phases θ_{jk} of the matrix V can be directly measured.

-
- [1] M. Reck, A. Zeilinger, H. J. Bernstein, and P. Bertani, *Phys. Rev. Lett.* **73**, 58 (1994).
 - [2] J. L. O’Brien, G. J. Pryde, A. Gilchrist, D. F. V. James, N. K. Langford, T. C. Ralph, and A. G. White, *Phys. Rev. Lett.* **93**, 080502 (2004).
 - [3] A. M. Childs, I. L. Chuang, and D. W. Leung, *Phys. Rev. A* **64**, 012314 (2001).
 - [4] M. W. Mitchell, C. W. Ellenor, S. Schneider, and A. M. Steinberg, *Phys. Rev. Lett.* **91**, 120402 (2003).
 - [5] M. Lobino, D. Korystov, C. Kupchak, E. Figueroa, B. C. Sanders, and A. I. Lvovsky, *Science* **322**, 563 (2008).

- [6] S. Rahimi-Keshari, A. Scherer, A. Mann, A. T. Reza-khani, A. I. Lvovsky, and B. C. Sanders, *New J. Phys.* **13**, 013006 (2011).
- [7] A. Shabani, R. L. Kosut, M. Mohseni, H. Rabitz, M. A. Broome, M. P. Almeida, A. Fedrizzi, and A. G. White, *Phys. Rev. Lett.* **106**, 100401 (2011).
- [8] G. VanWiggeren and D. Baney, *IEEE Photonics Technology Letters* **15**, 1267 (2003).
- [9] C. K. Hong, Z. Y. Ou, and L. Mandel, *Phys. Rev. Lett.* **59**, 2044 (1987).
- [10] A. Peruzzo, A. Laing, A. Politi, T. Rudolph, and J. L. O’Brien, *Nature Communications* **2**, 224 (2011).
- [11] A. Laing and J. L. O’Brien, *arXiv:1208.2868* (2012).
- [12] S. Aaronson and A. Arkhipov, *Proc. ACM Symposium on Theory of Computing*, San Jose, CA pp. 333-342 (2011).
- [13] A. Peres, *Nucl. Phys. B* **6**, 243 (1989).
- [14] H. J. Bernstein, *J. Math. Phys.* **15**, 1677 (1974).
- [15] Y. Bromberg, Y. Lahini, R. Morandotti, and Y. Silberberg, *Phys. Rev. Lett.* **102**, 253904 (2009).
- [16] R. Keil, A. Szameit, F. Dreisow, M. Heinrich, S. Nolte, and A. Tünnermann, *Phys. Rev. A* **81**, 023834 (2010).
- [17] K. Fan and A. J. Hoffman, *Proc. Amer. Math. Soc.* **6**, 11 (1955).
- [18] B. P. Lanyon, T. J. Weinhold, N. K. Langford, M. Barbieri, D. F. V. James, A. Gilchrist, and A. G. White, *Phys. Rev. Lett.* **99**, 250505 (2007).
- [19] B. Lanyon, J. Whitfield, G. Gillett, M. Goggin, M. Almeida, I. Kassal, J. Biamonte, M. Mohseni, B. Powell, M. Barbieri, A. Aspuru-Guzik, and A. G. White, *Nature Chemistry* **2**, 106 (2010).
- [20] A. Schreiber, A. Gábris, P. P. Rohde, K. Laiho, M. Štefaňák, V. Potoček, C. Hamilton, I. Jex, and C. Silberhorn, *Science* **336**, 55 (2012).
- [21] A. Peruzzo, M. Lobino, J. Matthews, N. Matsuda, A. Politi, K. Poulios, X. Zhou, Y. Lahini, N. Ismail, K. Wörhoff, Y. Bromberg, Y. Silberberg, M. G. Thompson, and J. L. O’Brien, *Science* **329**, 1500 (2010).
- [22] L. Sansoni, F. Sciarrino, G. Vallone, P. Mataloni, A. Crespi, R. Ramponi, and R. Osellame, *Phys. Rev. Lett.* **108**, 010502 (2012).
- [23] J. O. Owens, M. A. Broome, D. N. Biggerstaff, M. E. Goggin, A. Fedrizzi, T. Linjordet, M. Ams, G. D. Marshall, J. Twamley, M. J. Withford, and A. G. White, *New J. Phys.* **13**, 075003 (2011).
- [24] A. Sharkawy, S. Shi, D. Prather, and R. Soref, *Opt. Express* **10**, 1048 (2002).